

# Synthesis, crystal structure and X-ray powder diffraction data of the phosphor matrix $4\text{SrO}\cdot 7\text{Al}_2\text{O}_3$

DONG WANG\*, MINQUAN WANG

Materials Department, Zhejiang University, Hangzhou 310027, People's Republic of China  
E-mail: fu.jian@usa.net

GUANGLIE LÜ

Central Laboratory, Hangzhou University, Hangzhou 310028, People's Republic of China

The white phosphor matrix  $4\text{SrO}\cdot 7\text{Al}_2\text{O}_3$  has been synthesized by firing the appropriate mixture of  $\text{SrCO}_3$ ,  $\text{Al}(\text{OH})_3$  and  $\text{H}_3\text{BO}_3$  in the molar ratios 1:3.5:0.135 at  $1300^\circ\text{C}$  for 4–7 h. The crystal structure of  $4\text{SrO}\cdot 7\text{Al}_2\text{O}_3$  has been determined as a orthorhombic Pmma space group with  $a = 24.7451(2)\text{Å}$ ,  $b = 8.4735(6)\text{Å}$ ,  $c = 4.8808(1)\text{Å}$ ,  $V = 1023.41(3)\text{Å}^3$ ,  $Z = 2$ , and  $D = 3.66\text{ g cm}^{-3}$  by the Rietveld analysis. The refinement figures of merit are  $R_p = 8.26$ ,  $R_{\text{wp}} = 11.60$ ,  $R_{\text{bragg}} = 4.44$  and  $s = 2.61$  for 844 reflections with  $2\theta < 119.94^\circ$ . And the corresponding X-ray powder diffraction data are presented for search/match analysis.

© 1999 Kluwer Academic Publishers

## 1. Introduction

As a kind of new blue-green phosphor with high efficiency and good stableness for lamp, the aluminate phosphors activated by  $\text{Eu}^{2+}$  have been studied and applied widespreadly [1–3]. In 1983, Van Kemenade and Hoeks [4] reported that  $4\text{SrO}\cdot 7\text{Al}_2\text{O}_3:\text{Eu}^{2+}$  phosphor had higher quantum efficiency and better long-persistence properties than those of traditional aluminate and sulfide phosphors, which made  $4\text{SrO}\cdot 7\text{Al}_2\text{O}_3:\text{Eu}^{2+}$  a subject of more studies [5, 6]. According to the fluorescence spectra, the strong broad absorption bands of  $\text{Eu}^{2+}$  in  $4\text{SrO}\cdot 7\text{Al}_2\text{O}_3$  have been attributed to  $4f^7(^8\text{S}_{7/2}) \rightarrow 4f^65d$  transition. The energy of the promoted 5d electrons is strongly perturbed by its surroundings; changes in this level are responsible for the effects of host lattice and pressure on the optical properties of  $\text{Eu}^{2+}$ -doped materials. Except for the former soviet scholars T. N. Nadzhina *et al.* [7] have reported the structure of  $\text{Sr}_4\text{Al}_4\text{O}_2[\text{Al}_{10}\text{O}_{23}]$  single-crystal synthesized by the hydro-thermal method, there are few reports about the description and characterization of the structure of  $4\text{SrO}\cdot 7\text{Al}_2\text{O}_3$  compound. It was known, however, that almost all of  $4\text{SrO}\cdot 7\text{Al}_2\text{O}_3:\text{Eu}^{2+}$  phosphors were prepared by solid-state reaction method at rather high temperature (for example,  $1400\text{--}1600^\circ\text{C}$ ). So in view of economical coefficient and development, how to lower the preparing temperature of  $4\text{SrO}\cdot 7\text{Al}_2\text{O}_3$  compound and how to characterize its structure have become the questions which should be resolved immediately.

This paper studies the probability of synthesizing single-phase  $4\text{SrO}\cdot 7\text{Al}_2\text{O}_3$  by solid-state reaction

method at  $1300^\circ\text{C}$ , and the determination of the structure are made by the Rietveld analysis. The high-quality X-ray diffraction data and structural description are given out. It contributes to the further research on the development of the high efficient and economic aluminate phosphors.

## 2. Experimental

### 2.1. Sample preparation

According to the nominal compositions of  $4\text{SrO}\cdot 7\text{Al}_2\text{O}_3$  compound, appropriate amounts of the starting materials which include  $\text{SrCO}_3(\text{AR})$ ,  $\text{Al}(\text{OH})_3(\text{AR})$  and a little flux  $\text{H}_3\text{BO}_3(\text{AR})$  in the molar ratios 1:3.5:0.135 were thoroughly mixed and ground in an agate ball mill for 4 h. And subsequently the mixture were pre-fired at  $1000^\circ\text{C}$  for 5 h, and ground in agate ball mill for 4 h, and the pre-fired and ground mixture was divided into three portions which were calcined at  $1300^\circ\text{C}$  for 1, 4 and 7 h respectively. The calcined samples were ground in agate mortar for 2 h to prepare the samples for the X-ray powder diffraction analysis.

### 2.2. Measurements

A-Rigaku D/max-3B X-ray diffractometer, used in a step-scan mode, was used to collect the power diffraction data. Instrument parameters are given in Table I. The samples were packed into a recessed glass support and continuously rotated during the data collection. A silicon standard (SRM 640b) was used to correct instrument aberration and sample displacement. Rietveld

\* Authors to whom all correspondence should be addressed.

TABLE I Instrument parameters

Goniometer	Horizontal Bragg-Brentano
Radiation	Copper
Power	40 kV × 35 mA
Monochromator	Diffacted beam curved graphite tuned to CuK $\alpha$
Detector	Scintillation
Scan range (2 $\theta$ )	6°–120°
Step size	0.02°/2 $\theta$
Count time	8 s/step
Temperature	25 ± 1 °C
External standard	Silicon NIST SRM 640b ( $a = 5.43094 \text{ \AA}$ )

analysis was performed on the data using the software WYRIET3.0, over the range 6°–120°/2 $\theta$ . A pseudo-Voigt peak shape function was employed; the crystal structure parameters given by T. N. Nadzhina *et al.* [7] were used as initial structure model and the background was defined by a fourth-polynomial in 2 $\theta$ . The residuals were calculated as following [8]:

$$R_p = 100 \sum_{i=1}^n |I_{oi} - I_{ci}| / \sum_{i=1}^n |I_{oi}|$$

$$R_{wp} = 100 \left\{ \sum_{i=1}^n w_i \cdot (I_{oi} - I_{ci})^2 / \sum_{i=1}^n w_i \cdot (I_{oi})^2 \right\}^{1/2}$$

$$R_{exp} = 100 \left\{ (w - p + c) / \sum_{i=1}^n w_i \cdot I_{oi} \right\}^{1/2}$$

$$S = R_{wp} / R_{exp}$$

$$R_{Bragg} = 100 \sum_{i=1}^n |I_{oi} - I_{ci}| / \sum_{i=1}^n I_{oi}$$

where,  $R_p$  is the pattern  $R$ -factor;  $R_{wp}$  is the weighted pattern  $R$ -factor;  $n$  is the total number of data points (“observation”);  $p$  is the number of parameters adjusted;  $c$  is the number of constraints applied;  $I_{oi}$  is the observed (gross) intensity at the  $i$ th step;  $I_{ci}$  is the calculated intensity at the  $i$ th step;  $w_i$  is the weight of the  $i$ th step.

### 3. Results and discussion

The samples are calcined at 1300 °C for 1, 4 and 7 h respectively to make research on the possibility that 4SrO·7Al<sub>2</sub>O<sub>3</sub> compounds are prepared at relatively low temperature by the solid-state reaction method. The XRD pattern of the samples calcined at 1300 °C for different sintering time are shown in the Fig. 1. It can be seen that besides a few diffraction peaks of SrO·Al<sub>2</sub>O<sub>3</sub> and SrO·6Al<sub>2</sub>O<sub>3</sub>, there appear lots of diffraction peaks which can't be determined with available data upon the JCPDS on the XRD pattern of the sample calcined for 1 h. And with the calcining time being prolonged, the number and intensity of the unknown peaks increase and become stronger gradually, but the diffraction peaks of previously formed SrO·Al<sub>2</sub>O<sub>3</sub> and SrO·6Al<sub>2</sub>O<sub>3</sub> decrease in succession till they disappear. According to the starting composition of sample and

TABLE II The crystal structure parameters from Rietveld refinement of orthorhombic 4SrO·7Al<sub>2</sub>O<sub>3</sub>  $a = 24.7451(2) \text{ \AA}$ ,  $b = 8.4735(6) \text{ \AA}$ ,  $c = 4.8808(1) \text{ \AA}$ ,  $V = 1023.41 \text{ \AA}^3$ ,  $D_x = 3.66 \text{ g cm}^{-3}$ ,  $Z = 2$ , S.G. = Pmma

Atom	$x/a$	$y/b$	$z/c$	$B$	$N$
Sr1	0.1379(1)	0.500	0.0346(5)	0.8228	0.5
Sr2	0.1210(1)	0	0.1154(5)	0.4640	0.5
Al1	0.1861(2)	0.1936(6)	0.6196(2)	0.7525	1.0
Al2	0.0661(2)	0.3218(7)	0.5126(1)	0.3900	1.0
Al3	0.25	0.2950(8)	0.1297(6)	0.6043	0.5
Al4	0	0.1675(9)	0	0.4336	0.5
Al5	0	0	0.5	0.4592	0.25
Al6	0	0.5	0	0.3223	0.25
O1	0.0424(3)	0.1638(1)	0.3295(3)	0.3320	1.0
O2	0.1378(3)	0.3173(1)	0.5013(9)	0.4499	1.0
O3	0.1916(3)	0.2285(1)	-0.0265(7)	0.7918	1.0
O4	0.25	0.2286(6)	0.4796(3)	2.0315	0.5
O5	0.0367(5)	0	0.8287(3)	0.8059	0.5
O6	0.0512(4)	0.5	0.3548(3)	0.3993	0.5
O7	0.1639(5)	0	0.5777(8)	0.4359	0.5
O8	0.0435(3)	0.3348(1)	0.8467(4)	0.3926	1.0
O9	0.25	0.5	0.1001(4)	1.6802	0.25

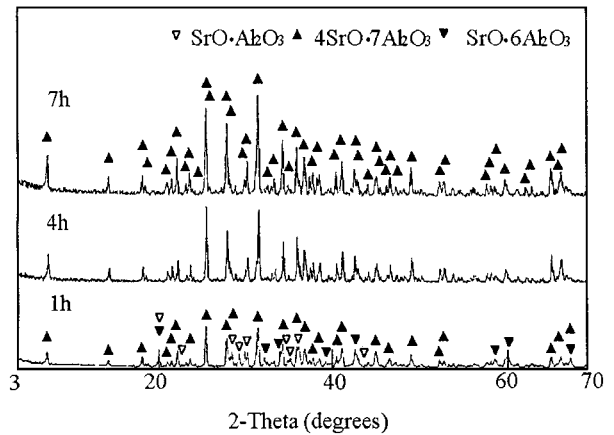
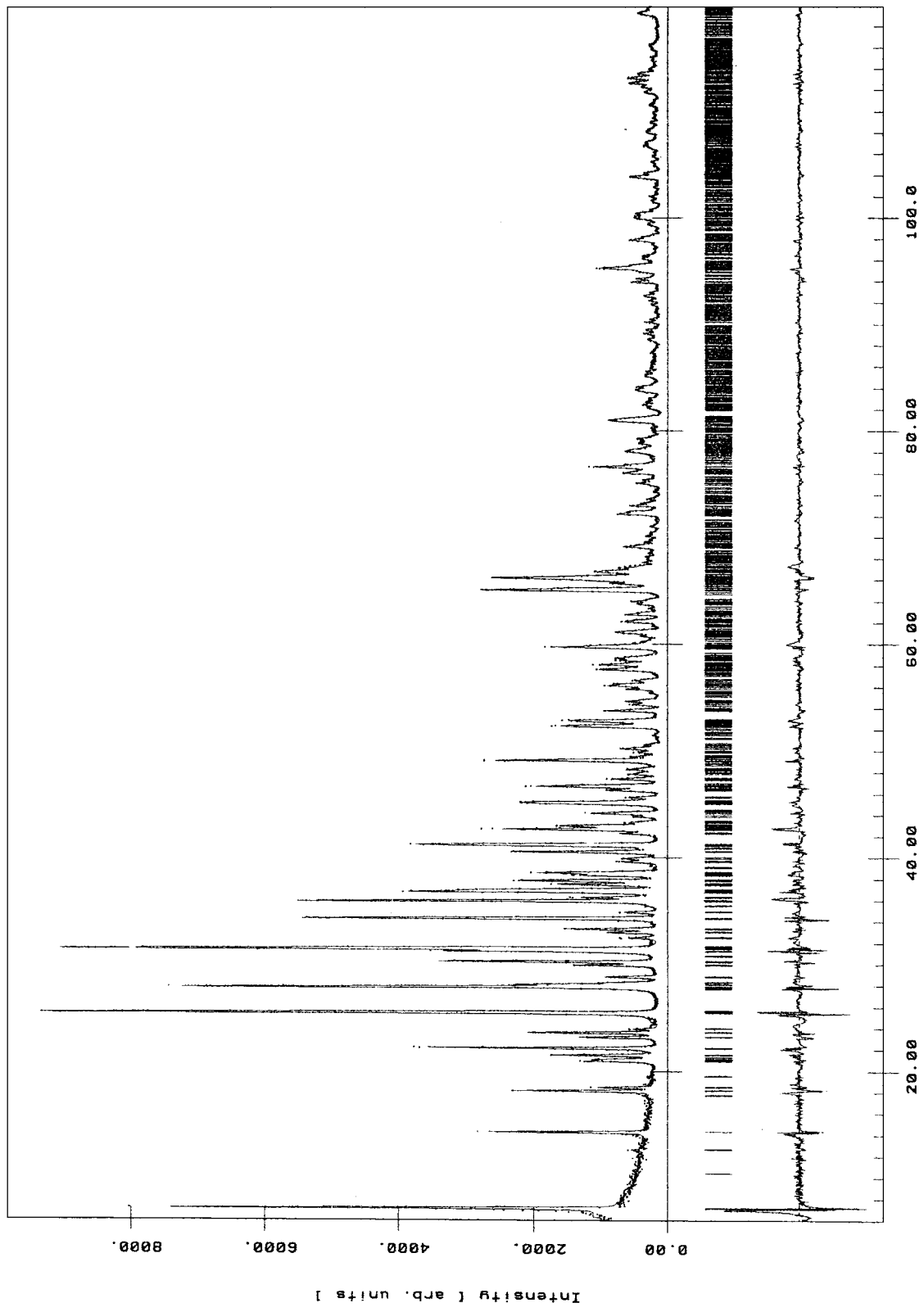


Figure 1 The XRD pattern of the samples calcined at 1300 °C for different time.

the rule of growth and decline of diffraction peaks, it is reasonable to consider that the unknown peaks are attributed to the forming of 4SrO·7Al<sub>2</sub>O<sub>3</sub>.

The crystal structure of the sample calcined at 1300 °C for 4 h is refined by Rietveld analysis to verify the forming of 4SrO·7Al<sub>2</sub>O<sub>3</sub>. The crystal structure parameters from the Rietveld refinements are presented in Table II. The corresponding diffraction profile is shown in Fig. 2, and the refinement figures of merit are  $R_p = 8.26$ ,  $R_{wp} = 11.60$ ,  $R_{bragg} = 4.44$  and  $S = 2.61$  for 844 reflections with  $2\theta < 119.4^\circ$ . From Fig. 2, it is obviously found that the calculated and the observed diffraction profile are not only the peak positions identical, but the relative peak intensities are similar to each other. Therefore, it is determined that 4SrO·7Al<sub>2</sub>O<sub>3</sub> compound can be synthesized at 1300 °C for 4–7 h by the solid-state reaction method and the crystal structure which crystallizes in the orthorhombic Pmma space group with  $a = 24.7451(2) \text{ \AA}$ ,  $b = 8.4735(6) \text{ \AA}$ ,  $c = 4.8808(1) \text{ \AA}$  was very similar to that synthesized by the hydro-thermal method.



2 - Theta [ degrees ]

Figure 2 The observed, calculated and difference X-ray diffraction profile for 4SrO·7Al<sub>2</sub>O<sub>3</sub> (The observed data are indicated by crosses and the calculated profile by the solid line. The short vertical lines below the profiles mark the position of all possible Bragg reflections).

TABLE III The calculated and observed powder diffraction data of orthorhombic 4SrO·7Al<sub>2</sub>O<sub>3</sub>

Observed			Calculated, $I/I_0$	$hkl$	$\Delta 2\theta$ (degrees)
$2\theta$ (degrees)	$I/I_0$	$d$ (Å)			
7.14	57	12.38	56	200	-0.004
14.32	21	6.19	21	400	+0.009
18.16	20	4.88	19	001	-0.006
18.52	8	4.79	8	101	+0.001
21.00	10	4.228	10	020,011	+0.007
21.14	7	4.200	8	301	+0.001
21.54	15	4.123	14	600	+0.006
22.18	37	4.006	36	220,211	+0.007
23.20	10	3.832	11	401	+0.001
23.64	19	3.761	20	311	+0.012
23.98	5	3.709	4	610	-0.003
25.48	96	3.494	95	420	+0.014
27.88	79	3.198	76	021	+0.013
28.12	20	3.171	20	121	+0.016
28.30	9	3.152	8	601	-0.013
28.84	9	3.094	9	800	-0.006
29.94	14	2.982	13	321	+0.004
30.26	36	2.952	36	620,611	+0.010
31.24	31	2.861	32	701	+0.018
31.46	100	2.842	100	421	+0.001
32.50	6	2.753	5	230	+0.006
33.00	9	2.713	8	711	-0.003
33.32	16	2.687	16	521	-0.004
34.30	62	2.613	64	801	.000
34.90	7	2.569	6	430	+0.004
35.92	61	2.498	60	820	-0.004
36.26	13	2.476	12	1000	-0.016
36.80	38	2.441	38	002,131	-0.004
36.98	25	2.429	24	102	-0.009
37.52	13	2.395	13	901	+0.001
37.86	24	2.375	24	1010	+0.009
38.38	13	2.344	13	012,331	+0.002
38.60	19	2.331	18	630	-0.009
39.68	5	2.270	4	402	+0.005
39.94	6	2.256	6	312	-0.001
40.54	26	2.224	27	821	+0.002
41.18	41	2.191	40	531,502	+0.001
42.30	5	2.135	6	1011	+0.014
42.66	30	2.118	29	512,040	+0.003
42.98	16	2.103	16	631,602	+0.001
43.32	4	2.087	4	240	+0.017
43.88	4	2.062	4	1200	+0.005
44.20	13	2.048	13	322	+0.016
45.08	26	2.010	25	731,702	+0.003
45.20	16	2.005	15	440,1210,422	+0.009
45.64	6	1.986	6	1111	-0.006
46.36	9	1.957	10	1021	+0.006
46.70	25	1.944	25	522,041	-0.001
46.86	3	1.937	3	141	-0.004
47.40	10	1.917	10	831,802	+0.002
47.86	6	1.899	6	1201	+0.007
48.10	2	1.890	2	341	+0.006
48.34	5	1.882	5	622	+0.006
49.10	35	1.854	34	1220,441,1211	+0.007
49.50	4	1.840	4	1121	-0.004
49.90	4	1.826	4	931,232	-0.001
50.26	8	1.814	7	722	+0.016
52.34	24	1.747	23	840,822	+0.008
52.82	12	1.732	12	1221	+0.007
53.80	12	1.703	12	741,1012	+0.014

TABLE III (Continued)

Observed			Calculated, $I/I_0$	$hkl$	$\Delta 2\theta$ (degrees)
$2\theta$ (degrees)	$I/I_0$	$d$ (Å)			
54.40	6	1.685	6	632	-0.002
54.72	7	1.676	7	922	.000
55.84	7	1.645	7	841	-0.009
56.16	8	1.637	8	732	-0.005
56.36	5	1.631	5	1420, 1411	-0.001
56.66	4	1.6233	4	103, 1112	+0.001
57.56	5	1.6001	5	042	-0.013
58.52	7	1.5761	7	1231	+0.005
58.76	3	1.5702	3	342	+0.010
58.86	2	1.5678	2	650	-0.012
59.74	21	1.5467	21	1421, 413, 1600	-0.010
59.99	4	1.5407	3	1122	+0.003
60.32	2	1.5333	2	932	-0.015
60.80	3	1.5220	4	542	-0.001
61.16	7	1.5142	7	603	-0.009
62.14	8	1.4927	8	323, 651	-0.004
62.84	6	1.4777	6	703	+0.009
63.82	3	1.4573	3	742	+0.003
64.08	4	1.4521	4	523	-0.006
65.08	37	1.4321	37	1431	+0.009
65.72	8	1.4197	8	813	-0.009
66.22	27	1.4102	27	033	-0.013
66.76	10	1.4001	10	233, 903	+0.002
67.19	7	1.3920	7	1621, 052	+0.012

$$\Delta 2\theta = 2\theta_{\text{Obs}} - 2\theta_{\text{Cal}}$$

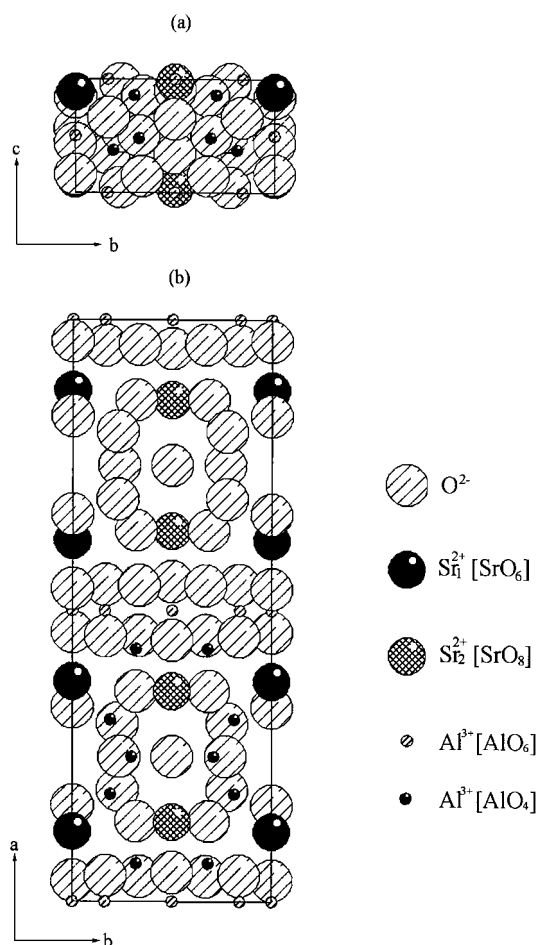


Figure 3 The projections of the unit cell of  $4\text{SrO}\cdot 7\text{Al}_2\text{O}_3$  viewed along the  $[100]^{(a)}$  and  $[001]^{(b)}$  directions.

The projections of the unit cell of  $4\text{SrO}\cdot 7\text{Al}_2\text{O}_3$  viewed along the  $[001]$  and  $[100]$  directions were shown in Fig. 3, where a twinned plane with mirror symmetry is found. According to the symmetry, the corresponding polyhedral drawing can be drawn to reflect the connective state of atoms in the cell (shown in Fig. 4). From Fig. 4, it is easy to find that the  $\text{AlO}_6$ -octahedra sharing the side form  $\text{AlO}_6$ -octahedral "walls" along the crystallographic  $b$ -axis in the  $bc$  plane; the  $\text{AlO}_6$ -octahedral "walls" are interconnected by  $\text{AlO}_4$ -tetrahedra which share the vertex each other; there are two different strontium sites in  $4\text{SrO}\cdot 7\text{Al}_2\text{O}_3$ ; the  $\text{Sr}_1$  site lies in the oxygen-polyhedron composed of six O atoms and the  $\text{Sr}_2$  site lies in the complicated oxygen-polyhedron composed of eight O atoms; through sharing the vertex, these two kinds of  $[\text{SrO}_n]$ -polyhedron were prolonged into a paralleling to  $b$ -axis line chain to strengthen the interconnection between  $[\text{AlO}_n]$ -polyhedron.

The crystal structure parameters, as determined by the Rietveld analysis, were used to compute a theoretical pattern and the calculated and observed X-ray data are listed in Table III. The identity of the calculated data with the observed data indicates that the calculated X-ray powder diffraction data of  $4\text{SrO}\cdot 7\text{Al}_2\text{O}_3$  are fit to make a determination.

#### 4. Conclusion

1.  $4\text{SrO}\cdot 7\text{Al}_2\text{O}_3$  compound can be prepared at  $1300^\circ\text{C}$  by the solid-state reaction method and its structure crystallizes in the orthorhombic  $\text{Pmma}$  space group with

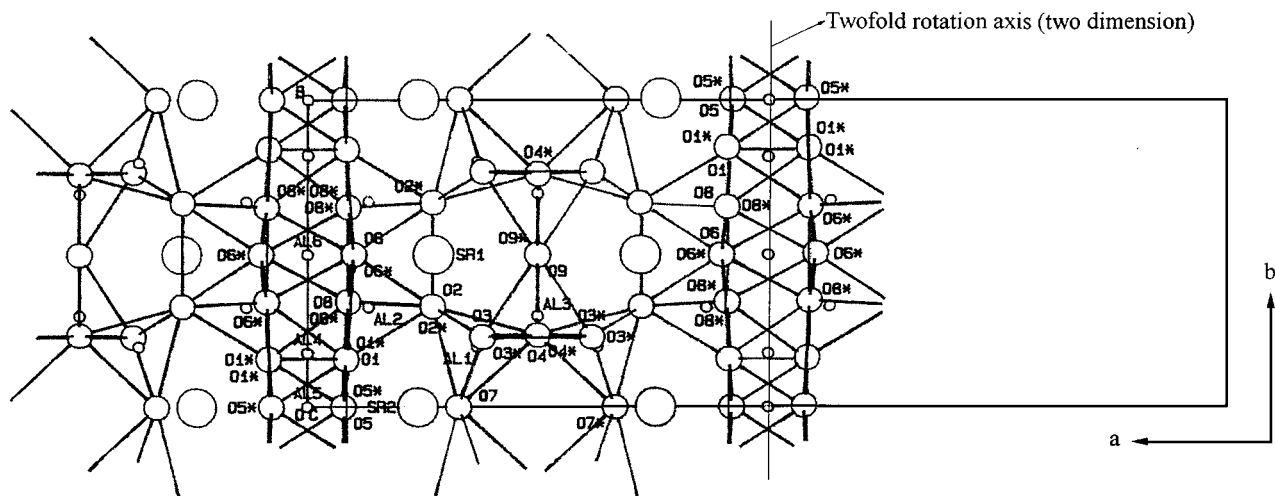


Figure 4 The polyhedral drawing which reflects the connective state of atoms in the cell.

$a = 24.7451(2) \text{ \AA}$ ,  $b = 8.4735(6) \text{ \AA}$ ,  $c = 4.8808(1) \text{ \AA}$ ,  
 $V = 1023.41(3) \text{ \AA}^3$ ,  $Z = 2$ , and  $D = 3.66 \text{ g cm}^{-3}$ .

2. The calculated X-ray powder diffraction data of  $4\text{SrO} \cdot 7\text{Al}_2\text{O}_3$  are accurate enough for search/match analysis.

### Acknowledgement

The project is supported by National Natural Science Foundation (No. 69890230).

### References

1. G. BLASSE and A. BRIL, *Philips Res. Repts.* **23** (1968) 201.
2. V. ABRUSCATO, *J. Electrochem. Soc.* **118**(6) (1971) 930.

3. B. SMETS, J. RUTTEN and G. HOEKS, *ibid.* **136**(7) (1989) 2119.
4. J. T. C. VAN KEMENADE and G. P. F. HOEKS, Abstract 607, 914, The Electrochemical Society Extended Abstracts, Vol. 83-1, San Francisco, CA, May 8-13, 1983.
5. YAMAMOTO KOSHI *et al.*, *Jpn. Kokai Tokkyo Koho JP* 63 191,886.
6. SONG QINGMEI *et al.*, *Optics* **12**(2) (1994) 144.
7. T. N. NADZHINA, E. A. POBEDIMSKAYA and N. V. BELOV, *Kristallografiya*, **25** (1980) 938.
8. R. A. YOUNG, "The Rietveld method," Oxford Science Publications, (London, 1993) p. 98.

Received 13 November 1998  
and accepted 7 April 1999